

Evidence for $B^+ \rightarrow \omega l^+ \nu$

C. Schwanda,⁹ K. Abe,⁶ K. Abe,³⁷ T. Abe,⁶ I. Adachi,⁶ H. Aihara,³⁹ M. Akatsu,¹⁹ Y. Asano,⁴³ T. Aushev,¹⁰ S. Bahinipati,³ A. M. Bakich,³⁴ Y. Ban,²⁸ E. Banas,²² A. Bay,¹⁵ I. Bizjak,¹¹ A. Bondar,¹ A. Bozek,²² M. Bračko,^{17,11} T. E. Browder,⁵ M.-C. Chang,²¹ Y. Chao,²¹ B. G. Cheon,³³ Y. Choi,³³ Y. K. Choi,³³ A. Chuvikov,²⁹ S. Cole,³⁴ M. Danilov,¹⁰ M. Dash,⁴⁵ L. Y. Dong,⁸ A. Drutskoy,¹⁰ S. Eidelman,¹ V. Eiges,¹⁰ N. Gabyshev,⁶ T. Gershon,⁶ G. Gokhroo,³⁵ B. Golob,^{16,11} M. Hazumi,⁶ I. Higuchi,³⁸ L. Hinz,¹⁵ T. Hokuue,¹⁹ Y. Hoshi,³⁷ W.-S. Hou,²¹ H.-C. Huang,²¹ T. Iijima,¹⁹ K. Inami,¹⁹ A. Ishikawa,⁶ R. Itoh,⁶ H. Iwasaki,⁶ M. Iwasaki,³⁹ J. H. Kang,⁴⁷ J. S. Kang,¹³ P. Kapusta,²² N. Katayama,⁶ H. Kawai,² H. Kichimi,⁶ H. J. Kim,⁴⁷ K. Kinoshita,³ P. Koppenburg,⁶ S. Korpar,^{17,11} P. Križan,^{16,11} P. Krokovny,¹ S. Kumar,²⁷ Y.-J. Kwon,⁴⁷ J. S. Lange,^{4,30} G. Leder,⁹ S. H. Lee,³² T. Lesiak,²² J. Li,³¹ A. Limosani,¹⁸ S.-W. Lin,²¹ J. MacNaughton,⁹ F. Mandl,⁹ T. Matsumoto,⁴¹ A. Matyja,²² Y. Mikami,³⁸ W. Mitaroff,⁹ H. Miyake,²⁶ H. Miyata,²⁴ T. Mori,⁴⁰ T. Nagamine,³⁸ Y. Nagasaka,⁷ E. Nakano,²⁵ M. Nakao,⁶ Z. Natkaniec,²² S. Nishida,⁶ O. Nitoh,⁴² T. Nozaki,⁶ S. Ogawa,³⁶ T. Ohshima,¹⁹ T. Okabe,¹⁹ S. Okuno,¹² S. L. Olsen,⁵ Y. Onuki,²⁴ W. Ostrowicz,²² H. Ozaki,⁶ P. Pakhlov,¹⁰ H. Palka,²² C. W. Park,¹³ H. Park,¹⁴ N. Parslow,³⁴ L. S. Peak,³⁴ L. E. Piilonen,⁴⁵ H. Sagawa,⁶ S. Saitoh,⁶ Y. Sakai,⁶ T. R. Sarangi,⁴⁴ O. Schneider,¹⁵ J. Schümann,²¹ A. J. Schwartz,³ S. Semenov,¹⁰ K. Senyo,¹⁹ M. E. Sevier,¹⁸ H. Shibuya,³⁶ J. B. Singh,²⁷ N. Soni,²⁷ R. Stamen,⁶ S. Stanič,^{43,*} M. Starič,¹¹ K. Sumisawa,²⁶ T. Sumiyoshi,⁴¹ S. Suzuki,⁴⁶ O. Tajima,³⁸ F. Takasaki,⁶ K. Tamai,⁶ M. Tanaka,⁶ Y. Teramoto,²⁵ T. Tomura,³⁹ T. Tsukamoto,⁶ S. Uehara,⁶ T. Uglov,¹⁰ K. Ueno,²¹ S. Uno,⁶ G. Varner,⁵ K. E. Varvell,³⁴ C. C. Wang,²¹ C. H. Wang,²⁰ B. D. Yabsley,⁴⁵ Y. Yamada,⁶ A. Yamaguchi,³⁸ Y. Yamashita,²³ H. Yanai,²⁴ J. Ying,²⁸ Z. P. Zhang,³¹ D. Žontar,^{16,11} and D. Zürcher¹⁵

(Belle Collaboration)

¹*Budker Institute of Nuclear Physics, Novosibirsk, Siberia*²*Chiba University, Chiba*³*University of Cincinnati, Cincinnati, Ohio 45221*⁴*University of Frankfurt, Frankfurt*⁵*University of Hawaii, Honolulu, Hawaii 96822*⁶*High Energy Accelerator Research Organization (KEK), Tsukuba*⁷*Hiroshima Institute of Technology, Hiroshima*⁸*Institute of High Energy Physics, Chinese Academy of Sciences, Beijing*⁹*Institute of High Energy Physics, Vienna*¹⁰*Institute for Theoretical and Experimental Physics, Moscow*¹¹*J. Stefan Institute, Ljubljana*¹²*Kanagawa University, Yokohama*¹³*Korea University, Seoul*¹⁴*Kyungpook National University, Taegu*¹⁵*Swiss Federal Institute of Technology of Lausanne, EPFL, Lausanne*¹⁶*University of Ljubljana, Ljubljana*¹⁷*University of Maribor, Maribor*¹⁸*University of Melbourne, Victoria*¹⁹*Nagoya University, Nagoya*²⁰*National United University, Miao Li, Taiwan*²¹*Department of Physics, National Taiwan University, Taipei, Taiwan*²²*H. Niewodniczanski Institute of Nuclear Physics, Krakow*²³*Nihon Dental College, Niigata*²⁴*Niigata University, Niigata*²⁵*Osaka City University, Osaka*²⁶*Osaka University, Osaka*²⁷*Panjab University, Chandigarh*²⁸*Peking University, Beijing*²⁹*Princeton University, Princeton, New Jersey 08545*³⁰*RIKEN BNL Research Center, Upton, New York 11973*³¹*University of Science and Technology of China, Hefei*³²*Seoul National University, Seoul*³³*Sungkyunkwan University, Suwon*³⁴*University of Sydney, Sydney NSW*

³⁵Tata Institute of Fundamental Research, Bombay³⁶Toho University, Funabashi³⁷Tohoku Gakuin University, Tagajo³⁸Tohoku University, Sendai³⁹Department of Physics, University of Tokyo, Tokyo⁴⁰Tokyo Institute of Technology, Tokyo⁴¹Tokyo Metropolitan University, Tokyo⁴²Tokyo University of Agriculture and Technology, Tokyo⁴³University of Tsukuba, Tsukuba⁴⁴Utkal University, Bhubaneswar⁴⁵Virginia Polytechnic Institute and State University, Blacksburg, Virginia 24061⁴⁶Yokkaichi University, Yokkaichi⁴⁷Yonsei University, Seoul

(Received 12 February 2004; published 23 September 2004)

We have searched for the decay $B^+ \rightarrow \omega l^+ \nu$ ($l = e$ or μ) in 78 fb^{-1} of $Y(4S)$ data ($85 \times 10^6 B\bar{B}$ events) accumulated with the Belle detector. The final state is fully reconstructed using the ω decay into $\pi^+ \pi^- \pi^0$, combined with detector hermeticity to estimate the neutrino momentum. A signal of 414 ± 125 events is found in the data, corresponding to a branching fraction of $(1.3 \pm 0.4 \pm 0.2 \pm 0.3) \times 10^{-4}$, where the first two errors are statistical and systematic, respectively. The third error reflects the estimated form-factor uncertainty.

DOI: 10.1103/PhysRevLett.93.131803

PACS numbers: 13.20.He, 12.15.Hh

The magnitude of V_{ub} plays an important role in probing the unitarity of the Cabibbo-Kobayashi-Maskawa (CKM) matrix [1]. The cleanest way to constrain this quantity is either by measuring the decay $B \rightarrow X_u l \nu$ [2] inclusively, or by reconstructing one of its exclusive submodes. As to the latter, the decay modes $B \rightarrow \pi l \nu$ and $B \rightarrow \rho l \nu$ have already been observed [3,4]. In this Letter, we present a study of the decay $B^+ \rightarrow \omega l^+ \nu$ [5], which has not been measured so far [6,7]. Using three different form-factor calculations, ISGW2 [8], UKQCD [9], and LCSR [10], we extrapolate the decay rates to the full range of lepton momentum and measure the branching fraction of this decay.

The analysis is based on the data recorded with the Belle detector [11] at the asymmetric e^+e^- collider KEKB [12] operating at the center-of-mass (c.m.) energy of the $Y(4S)$ resonance. KEKB consists of a low energy ring (LER) of 3.5 GeV positrons and a high energy ring (HER) of 8 GeV electrons. The $Y(4S)$ data set used for this study corresponds to an integrated luminosity of 78.1 fb^{-1} and contains $(85.0 \pm 0.5) \times 10^6 B\bar{B}$ events. In addition, 8.8 fb^{-1} of data taken at 60 MeV below the resonance are used to study the continuum (non- $B\bar{B}$) background.

The Belle detector is a large-solid-angle magnetic spectrometer consisting of a three-layer silicon vertex detector (SVD), a 50-layer central drift chamber (CDC), an array of aerogel threshold Čerenkov counters (ACC), a barrel-like arrangement of time-of-flight scintillation counters (TOF), and an electromagnetic calorimeter comprised of CsI(Tl) crystals (ECL) located inside a superconducting solenoid coil that provides a 1.5 T magnetic field. The responses of the ECL, CDC (dE/dx), and ACC detectors are combined to provide

clean electron identification. Muons are identified in the instrumented iron flux-return (KLM) located outside of the coil. Charged hadron identification relies on the information from the CDC, ACC, and TOF subdetectors.

Full detector simulation based on GEANT [13] is applied to Monte Carlo simulated events. This analysis uses background Monte Carlo samples equivalent to about 3 times the integrated luminosity. The decay $B \rightarrow D^* l \nu$ is simulated using a model based on Heavy Quark Effective Theory [14]. The ISGW2 model is used for the decays $B \rightarrow D l \nu$ and $B \rightarrow D^{**} l \nu$. The modes $B \rightarrow D^{(*)} \pi l \nu$ are simulated according to the Goity-Roberts model [15]. The ISGW2 and the De Fazio-Neubert model [16] are used to model the cross feed from other decays $B \rightarrow X_u l \nu$.

Events passing the hadronic selection [17] are required to contain a single lepton (electron or muon) with a c.m. momentum p_l^* [18] between 1.8 and 2.7 GeV/c. In this momentum range, electrons (muons) are selected with an efficiency of 92% (89%), and the probability to misidentify a pion as an electron (a muon) is 0.25% (1.4%) [19,20].

The missing four-momentum is calculated,

$$\begin{aligned} \vec{P}_{\text{miss}} &= \vec{P}_{\text{HER}} + \vec{P}_{\text{LER}} - \sum_i \vec{P}_i, \\ E_{\text{miss}} &= E_{\text{HER}} + E_{\text{LER}} - \sum_i E_i, \end{aligned} \quad (1)$$

where the sums run over all reconstructed charged tracks (assumed to have the pion mass) and photons, and the labels HER and LER refer to the two colliding beams. To reject events in which the missing momentum misrepresents the neutrino momentum, the following requirements are applied. The total event charge must be close

to neutral: $|Q_{\text{tot}}| < 3e$; the polar angle of the missing momentum (with respect to the beam direction) is required to lie within the ECL acceptance: $17^\circ < \theta_{\text{miss}} < 150^\circ$; and the missing mass squared, $m_{\text{miss}}^2 = E_{\text{miss}}^2 - \vec{p}_{\text{miss}}^2$, is required to be zero within about ± 3 standard deviations: $|m_{\text{miss}}^2| < 3 \text{ GeV}^2/c^4$.

For generic $B \rightarrow X_u l \nu$ events, the efficiency after applying these requirements is 11%, and the resolution in the magnitude of the missing momentum is around $140 \text{ MeV}/c$. As the missing energy resolution is worse than the missing momentum resolution, the neutrino four-momentum is taken to be $(|\vec{p}_{\text{miss}}|, \vec{p}_{\text{miss}})$.

Pairs of photons satisfying $E_\gamma > 30 \text{ MeV}$, $p_{\pi^0}^* > 200 \text{ MeV}/c$, and $120 \text{ MeV}/c^2 < m(\gamma\gamma) < 150 \text{ MeV}/c^2$ are combined to form π^0 candidates. The decay $\omega \rightarrow \pi^+ \pi^- \pi^0$ is reconstructed using all possible combinations of one π^0 with two oppositely charged tracks. Combinations with a charged track identified as a kaon are rejected, and the following requirements are imposed: $p_\omega^* > 300 \text{ MeV}/c$, $703 \text{ MeV}/c^2 < m(\pi^+ \pi^- \pi^0) < 863 \text{ MeV}/c^2$. The Dalitz amplitude, $A \propto |\vec{p}_{\pi^+} \times \vec{p}_{\pi^-}|$, is required to be larger than half of its maximum value.

The lepton in the event is combined with the ω candidate and the neutrino. To reject combinations inconsistent with signal decay kinematics, the requirement $|\cos\theta_{BY}| < 1.1$ is imposed, where

$$\cos\theta_{BY} = \frac{2E_B^* E_Y^* - m_B^2 - m_Y^2}{2p_B^* p_Y^*}, \quad (2)$$

and E_B^* , p_B^* , and m_B are fixed to $E_{\text{beam}}^* = \sqrt{E_{\text{HER}} E_{\text{LER}}}$, $\sqrt{E_B^{*2} - m_B^2}$, and $5.279 \text{ GeV}/c^2$, respectively. The variables E_Y^* , p_Y^* , and m_Y are the measured c.m. energy, momentum, and mass of the $Y = \omega + l$ system, respectively. For well-reconstructed signal events, $\cos\theta_{BY}$ is the cosine of the angle between the B and the Y system and lies between -1 and $+1$ while for background, the majority of events are outside this interval.

For each $B^+ \rightarrow \omega l^+ \nu$ candidate, the beam-energy constrained mass M_{bc} and ΔE are calculated,

$$M_{\text{bc}} = \sqrt{(E_{\text{beam}}^*)^2 - |\vec{p}_\omega^* + \vec{p}_l^* + \vec{p}_\nu^*|^2}, \quad (3)$$

$$\Delta E = (E_\omega^* + E_l^* + E_\nu^*) - E_{\text{beam}}^*,$$

and candidates in the range $M_{\text{bc}} > 5.23 \text{ GeV}/c^2$ and $|\Delta E| < 1.08 \text{ GeV}$ are selected. On average, 2.5 combinations per event satisfy all selection criteria, and we choose the one with the largest ω momentum in the c.m. frame. Monte Carlo simulation indicates that this choice is correct in 77% of the signal cases.

In $B\bar{B}$ events, the two B mesons are produced nearly at rest, and their decay products are uniformly distributed over the solid angle in the c.m. frame. Conversely, continuum events have a jetlike topology. We exploit this property to suppress continuum background with the following quantities (defined in the c.m. frame): the ratio R_2 of the second to the zeroth Fox-Wolfram moment [21] which tends to be close to zero (unity) for spherical (jetlike) events; $\cos\theta_{\text{thrust}}$, where θ_{thrust} is the angle between the thrust axis of the ωl system and the thrust axis of the rest of the event; and a Fisher discriminant [22] that selects events with a uniform energy distribution around the lepton direction. The input variables to the latter are the charged and neutral energy in nine cones of equal solid angle around the lepton momentum axis. The selection $\mathcal{L}_S/(\mathcal{L}_S + \mathcal{L}_B) > 0.9$ is applied, where \mathcal{L}_S (\mathcal{L}_B) is the product of the signal (background) probability density functions of these three quantities. This selection is 56% efficient for signal decays and eliminates 92% of the remaining continuum background.

The signal yield is determined by a three-dimensional binned maximum likelihood fit taking into account finite Monte Carlo statistics [23]. We use nine 240 MeV wide bins in ΔE , eight $20 \text{ MeV}/c^2$ wide bins of $m(\pi^+ \pi^- \pi^0)$, and three $300 \text{ MeV}/c$ wide p_l^* bins. The signal resolutions in ΔE and $m(\pi^+ \pi^- \pi^0)$ are about 140 MeV and $11 \text{ MeV}/c^2$, respectively. The backgrounds from the remaining continuum events and from $B\bar{B}$ events in which the lepton is misidentified or does not originate directly from a B decay are subtracted from the raw yield bin-by-

TABLE I. The result of the fit assuming ISGW2 form factors for $B^+ \rightarrow \omega l^+ \nu$. The uncertainties quoted are statistical only.

	p_l^* range (GeV/c):			
	1.8–2.1	2.1–2.4	2.4–2.7	1.8–2.7
Raw yield	16 777	4639	326	21 742
Continuum	234 ± 45	294 ± 50	78 ± 26	606 ± 72
Other bkgd.	211 ± 9	216 ± 9	28 ± 3	455 ± 13
Subtr. yield	$16\,332 \pm 46$	4129 ± 51	220 ± 26	$20\,681 \pm 74$
$B^+ \rightarrow \omega l^+ \nu$	101 ± 31	193 ± 59	89 ± 28	383 ± 118
$B \rightarrow X_u l \nu$	339 ± 151	466 ± 142	125 ± 19	930 ± 312
$B \rightarrow X_c l \nu$	$15\,755 \pm 238$	3592 ± 64	0	$19\,348 \pm 289$
Sum	$16\,196 \pm 284$	4251 ± 166	215 ± 34	$20\,662 \pm 442$

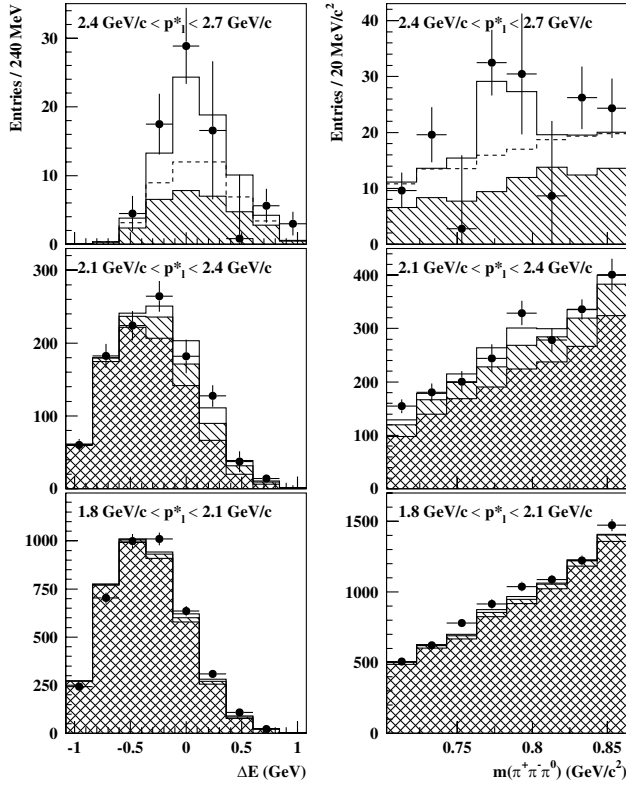


FIG. 1. The ΔE and $m(\pi^+ \pi^- \pi^0)$ projections of the fit assuming ISGW2 form factors for $B^+ \rightarrow \omega l^+ \nu$ after requiring $763 \text{ MeV}/c^2 < m(\pi^+ \pi^- \pi^0) < 803 \text{ MeV}/c^2$ and $|\Delta E| < 360 \text{ MeV}$, respectively. The data points are the background subtracted yields. The open, hatched, and doubly-hatched histograms correspond to the $B^+ \rightarrow \omega l^+ \nu$ signal, the $B \rightarrow X_u l \nu$ background, and the $B \rightarrow X_c l \nu$ background, respectively. In the highest momentum bin, the contribution of signal candidates in which the lepton stems from a $B^+ \rightarrow \omega l^+ \nu$ decay but the ω is reconstructed improperly is shown by the dashed histogram.

bin. The continuum background is estimated using the off-resonance data (scaled to the on-resonance luminosity). The fake and nonprimary lepton backgrounds (which account for only about 2% of the raw yield) are determined from the simulation. The signal yield, the background from $B \rightarrow X_u l \nu$ decays and the background from $B \rightarrow X_c l \nu$ decays are fitted after this subtraction. In the region defined by $763 \text{ MeV}/c^2 < m(\pi^+ \pi^- \pi^0) <$

$803 \text{ MeV}/c^2$, $|\Delta E| < 360 \text{ MeV}$ the signal purity is almost 3 times higher than the average in the whole fitting space; the broader fit ranges in ΔE , $m(\pi^+ \pi^- \pi^0)$ permit a reliable determination of the signal and background components. The distribution shapes of the three fit components are taken from Monte Carlo simulation. The contribution of each component is described by a single parameter.

Table I and Fig. 1 show the result of the fit assuming ISGW2 form factors for $B^+ \rightarrow \omega l^+ \nu$. We find 383 ± 118 signal events with a statistical significance of 3.8 standard deviations. The latter is defined as $\sqrt{-2 \ln(\mathcal{L}_B/\mathcal{L}_{S+B})}$, where \mathcal{L}_{S+B} (\mathcal{L}_B) refers to the maximum of the likelihood function describing signal and background (background only). In addition to well-reconstructed signal decays, the signal component of the fit also includes candidates in which the lepton stems from a $B^+ \rightarrow \omega l^+ \nu$ decay but the ω failed to be reconstructed properly. This subcomponent is shown separately in Fig. 1. It scales with the actual signal and amounts to 36% of the signal component within the $763 \text{ MeV}/c^2 < m(\pi^+ \pi^- \pi^0) < 803 \text{ MeV}/c^2$, $|\Delta E| < 360 \text{ MeV}$ region.

The fit is repeated for the three form-factor models considered for $B^+ \rightarrow \omega l^+ \nu$. For each model, the signal yield $N(B^+ \rightarrow \omega l^+ \nu)$ is determined and the branching fraction $\mathcal{B}(B^+ \rightarrow \omega l^+ \nu)$ is calculated according to the relation $N(B^+ \rightarrow \omega l^+ \nu) = N(B^+) \times \mathcal{B}(B^+ \rightarrow \omega l^+ \nu) \times \mathcal{B}(\omega \rightarrow \pi^+ \pi^- \pi^0) \times (\epsilon_e + \epsilon_\mu)$, where $N(B^+)$ is the total number of charged B mesons in the data (assumed to be equal to the number of $B\bar{B}$ events), $\mathcal{B}(\omega \rightarrow \pi^+ \pi^- \pi^0) = (89.1 \pm 0.7)\%$ [24], and ϵ_e (ϵ_μ) is the model-dependent selection efficiency for $\omega e \nu$ ($\omega \mu \nu$) signal candidates. The results are presented in Table II. Averaging the central values and the statistical uncertainties over the three models (giving equal weight to each), a branching fraction of $(1.3 \pm 0.4) \times 10^{-4}$ is obtained. The spread around this average value amounts to 0.3×10^{-4} , and provides an estimate of the form-factor model uncertainty.

The experimental systematic error is 18.1% of the branching fraction (Table III), or 0.2×10^{-4} in absolute. The largest contribution is the uncertainty in the $X_u l \nu$ cross feed. It is estimated by separately varying the fraction of $B \rightarrow \pi l \nu$ and $B \rightarrow \rho l \nu$ decays (which are

TABLE II. The fitted signal yield, the selection efficiency for signal candidates, the branching fraction and the goodness of fit (estimated by the χ^2 divided by the number of degrees of freedom). For each fit (using a given form-factor model), the error quoted on the signal yield and the branching fraction is statistical only. For the average, the first error is statistical, and the second is the spread around the central value.

Form-factor model	$N(B^+ \rightarrow \omega l^+ \nu)$	$\epsilon_e + \epsilon_\mu$	$\mathcal{B}(B^+ \rightarrow \omega l^+ \nu)/10^{-4}$	χ^2/ndf
ISGW2 [8]	383 ± 118	5.0%	1.0 ± 0.3	1.05
UKQCD [9]	384 ± 116	4.2%	1.2 ± 0.4	1.08
LCSR [10]	473 ± 141	3.8%	1.7 ± 0.5	1.04
Average	$414 \pm 125 \pm 42$		$1.3 \pm 0.4 \pm 0.3$	

TABLE III. Contributions to the systematic uncertainty. The size of each contribution is given as percentage of the branching fraction.

	$\Delta\mathcal{B}/\mathcal{B}$
$B \rightarrow \pi l \nu$ cross feed	2.2%
$B \rightarrow \rho l \nu$ cross feed	14.8%
Other $B \rightarrow X_u l \nu$ cross feed	1.4%
(Sum)	15.1%
Neutrino reconstruction	4%
Charged track finding (l, π^+, π^-)	3%
Cluster finding (π^0)	4%
(Sum)	9%
$X_c l \nu$ cross feed	2.7%
Lepton identification	3.0%
Number of $B\bar{B}$	0.6%
$\omega \rightarrow \pi^+ \pi^- \pi^0$ branching fraction [24]	0.8%
Total systematic uncertainty	18.1%

expected to dominate in the high p_l^* region) within their respective experimental uncertainties [24]. The relative fractions of charged and neutral modes are constrained using isospin symmetry. For the $B \rightarrow \rho l \nu$ mode, we also consider the form-factor model dependence of the cross feed [8–10]. To estimate the uncertainty in the cross feed from other $B \rightarrow X_u l \nu$ decays, the fit is repeated modeling this component once with ISGW2, and once with the De Fazio-Neubert model. Half of the difference between these two cases is assigned as a systematic uncertainty. The next-to-largest component is the uncertainty in the neutrino reconstruction, track finding, and cluster finding efficiency. While the latter two are uncorrelated, they are treated as fully correlated with the former. The $X_c l \nu$ cross feed uncertainty is estimated by varying the fractions of $B \rightarrow D^* l \nu$, $B \rightarrow D l \nu$, and $B \rightarrow D^{**}/D^{(*)} \pi l \nu$ in $B \rightarrow X_c l \nu$ within $\pm 10\%$, $\pm 10\%$, and $\pm 30\%$, respectively, and summing the individual variations in quadrature.

In summary, we have measured the $B^+ \rightarrow \omega l^+ \nu$ branching fraction to be $[1.3 \pm 0.4(\text{stat}) \pm 0.2(\text{syst}) \pm 0.3(\text{model})] \times 10^{-4}$, based on 414 ± 125 signal events. This is the first evidence for this decay. Assuming the quark model relation $\Gamma(B^0 \rightarrow \rho^- l^+ \nu) = 2\Gamma(B^+ \rightarrow \omega l^+ \nu)$, our measurement agrees with measurements of the decay $B^0 \rightarrow \rho^- l^+ \nu$ [3,4].

We thank the KEKB group for the excellent operation of the accelerator, the KEK Cryogenics group for the efficient operation of the solenoid, and the KEK computer group and the NII for valuable computing and SuperSINET network support. We acknowledge support from MEXT and JSPS (Japan); ARC and DEST (Australia);

NSFC (Contract No. 10175071, China); DST (India); the BK21 program of MOEHRD and the CHEP SRC program of KOSEF (Korea); KBN (Contract No. 2P03B 01324, Poland); MIST (Russia); MESS (Slovenia); NSC and MOE (Taiwan); and DOE (USA).

*On leave from Nova Gorica Polytechnic, Nova Gorica

- [1] M. Kobayashi and T. Maskawa, *Prog. Theor. Phys.* **49**, 652 (1973).
- [2] Throughout this letter, X_u (X_c) refers to a hadron or hadronic system containing a u -quark (c -quark) and (a) light spectator(s).
- [3] CLEO Collaboration, S. B. Athar *et al.*, *Phys. Rev. D* **68**, 072003 (2003).
- [4] BABAR Collaboration, B. Aubert *et al.*, *Phys. Rev. Lett.* **90**, 181801 (2003).
- [5] Throughout this Letter, the inclusion of the charge conjugate mode is implied.
- [6] ARGUS Collaboration, H. Albrecht *et al.*, *Phys. Lett.* **B255**, 297 (1991).
- [7] CLEO Collaboration, A. Bean *et al.*, *Phys. Rev. Lett.* **70**, 2681 (1993).
- [8] N. Isgur and D. Scora, *Phys. Rev. D* **52**, 2783 (1995); See also N. Isgur *et al.*, *Phys. Rev. D* **39**, 799 (1989).
- [9] L. Del Debbio *et al.*, *Phys. Lett.* **B416**, 392 (1998).
- [10] P. Ball and V.M. Braun, *Phys. Rev. D* **58**, 094016 (1998).
- [11] Belle Collaboration, A. Abashian *et al.*, *Nucl. Instrum. Methods Phys. Res., Sect. A* **479**, 117 (2002).
- [12] S. Kurokawa and E. Kikutani, *Nucl. Instrum. Methods Phys. Res., Sect. A* **499**, 1 (2003), and other papers included in this volume.
- [13] R. Brun *et al.*, CERN Report No. DD/EE/84-1, GEANT 3.21, (1984).
- [14] CLEO Collaboration, J. Duboscq *et al.*, *Phys. Rev. Lett.* **76**, 3898 (1996).
- [15] J. L. Goity and W. Roberts, *Phys. Rev. D* **51**, 3459 (1995).
- [16] F. De Fazio and M. Neubert, *J. High Energy Phys.* 06 (1999) 017.
- [17] The selection of hadronic events is described in Belle Collaboration, K. Abe *et al.*, *Phys. Rev. D* **64**, 072001 (2001).
- [18] Throughout this Letter, quantities calculated in the c.m. frame are denoted by an asterisk.
- [19] K. Hanagaki *et al.*, *Nucl. Instrum. Methods Phys. Res., Sect. A* **485**, 490 (2002).
- [20] A. Abashian *et al.*, *Nucl. Instrum. Methods Phys. Res., Sect. A* **491**, 69 (2002).
- [21] G.C. Fox and S. Wolfram, *Phys. Rev. Lett.* **41**, 1581 (1978).
- [22] R. A. Fisher, *Annals of Eugenics* **7**, 179 (1936).
- [23] R. Barlow and C. Beeston, *Comput. Phys. Commun.* **77**, 219 (1993).
- [24] K. Hagiwara *et al.*, *Phys. Rev. D* **66**, 010001 (2002).